NASA MEMO 2-11-59E

NASA

MEMORANDUM

EFFECT OF STATOR AND ROTOR ASPECT RATIO ON TRANSONIC-TURBINE PERFORMANCE

By Robert Y. Wong and Daniel E. Monroe

Lewis Research Center
Cleveland, Ohio

NATIONAL AERONAUTICS AND SPACE ADMINISTRATION
WASHINGTON
February 1959

NATIONAL AERONAUTICS AND SPACE ADMINISTRATION

MEMORANDUM 2-11-59E

EFFECT OF STATOR AND ROTOR ASPECT RATIO ON TRANSONIC-TURBINE PERFORMANCE

By Robert Y. Wong and Daniel E. Monroe

SUMMARY

The effect of stator and rotor aspect ratio on transonic-turbine performance was experimentally investigated. The stator aspect ratios covered were 1.6, 0.8, and 0.4, while the rotor aspect ratios investigated were 1.46 and 0.73. It was found that the observed variation in turbine design-point efficiency was negligible. Thus, within the range of aspect ratio investigated, these results verify for turbines operating in the transonic flow range the finding of a reference report, which showed analytically that, if blade shape and solidity are held constant, the aspect ratio may be varied over a wide range without appreciable change in turbine efficiency.

INTRODUCTION

In the design of a turbine it is in many cases desirable to select the aspect ratio of the blading from such mechanical considerations as turbine weight, disk stress, or blade manufacturing tolerances. Therefore, it is important that the designer understand the significance of his selection on the resultant over-all turbine performance.

Recent analytical investigations into losses occurring in turbomachinery have indicated that, if surface velocity distributions are maintained constant (by maintaining blade shape and solidity of blades in a blade row), the aspect ratio may be varied over a wide range without appreciable change in over-all turbine loss (ref. 1). This result was experimentally verified with reference 2 for turbines designed for conservative velocity diagrams.

The investigation described in this report determines if the aspect ratio effects predicted in reference 1 can be applied to turbines operating in the transonic flow range. Three transonic stators were

investigated experimentally, each with the same rotor. The stator aspect ratios selected were 1.6, 0.8, and 0.4 with both the stator blade shape and solidity held constant. In addition, two transonic rotors having aspect ratios of 1.46 and 0.73 were investigated using the highest aspect ratio stator. The latter one was used in the stator study. The manner used in varying the rotor aspect ratio was the same as that used for the stator. Included in this report are the results of the over-all performance tests of the four turbines investigated. In addition, the results of surveys obtained behind the three stators are presented to further establish the fundamental reasons as to why the observed aspect ratio effects occurred.

SYMBOLS

$\mathscr{A}$	aspect ratio, $\frac{\text{blade height}}{\text{chord length}}$
c	chord length, ft
H_w	blade wake form factor, ratio of wake displacement thickness to wake momentum thickness
$\Delta h'$	specific work output, Btu/lb
N	rotative speed, rpm
n	exponent used to describe simple boundary-layer velocity profile
p	pressure, lb/sq ft
r	radius
U	blade velocity, ft/sec
V	absolute gas velocity, ft/sec
W	relative gas velocity, ft/sec
w	weight flow, lb/sec
γ	ratio of specific heats
δ	ratio of inlet total pressure to NASA standard sea-level pressure, p'_0/p^*

ϵ $$\frac{\gamma^*}{\gamma}\left[\frac{\left(\frac{\gamma+1}{2}\right)^{\frac{\gamma}{\gamma-1}}}{\left(\frac{\gamma^*+1}{2}\right)^{\frac{\gamma^*}{\gamma^*-1}}}\right]$$

η adiabatic efficiency defined as ratio of turbine work based on torque, weight flow, and speed measurements to ideal work based on inlet total temperature and inlet and outlet total pressure, both defined as sum of static pressure plus pressure corresponding to gas velocity

Θ_{cr} squared ratio of critical velocity at turbine inlet to critical velocity at NASA standard sea-level temperature, $(V_{cr,0}/V^*_{cr})^2$

θ_w blade wake momentum thickness, ft

Subscripts:

cr conditions at Mach number of 1.00

fs conditions at free stream or that region between blade wakes

le leading edge

t tip

te trailing edge

x axial direction

0 upstream of stator (see fig. 2)

1 channel exit

2 station just upstream of stator trailing edge

3 station in free stream between stator and rotor

5 station just upstream of rotor trailing edge

6 downstream of rotor

Superscripts:

$*$ NASA standard conditions

$'$ absolute total state

TURBINE DESIGN

Design Requirements

The following design requirements for the 14-inch cold-air turbines investigated herein are the same as reference 3:

Equivalent specific work, $\Delta h'/\Theta_{cr}$, Btu/lb 22.61

Equivalent weight flow, $\epsilon w\sqrt{\Theta_{cr}}/\delta$, lb/sec 11.95

Equivalent tip speed, $U_t/\sqrt{\Theta_{cr}}$, ft/sec 597

Stator Design

The three stator blade rows used in this investigation were obtained by using the stator blade described in reference 3 and scaling the profiles of this stator to one-half and twice the size, while maintaining the solidity at 1.41 (defined herein as the ratio of chord to spacing at the mean radius) and the blade height at 2.1 inches. This resulted in the three stator blade rows containing 40, 20, and 10 blades. The 40-, 20-, and 10-blade stators with corresponding aspect ratios (A) of 1.6, 0.8, and 0.4 will be hereafter referred to as stators A, B, and C, respectively. The aspect ratios and number of blades for the three stators are tabulated in table I.

The trailing-edge radii of the stators were maintained at 0.005 inch. The spacing changes due to aspect-ratio variations while maintaining trailing-edge thickness and solidity constant resulted in a variation in trailing-edge blockage, which in turn resulted in slightly different blade velocity diagrams as tabulated in table II. The coordinates on cylindrical surfaces for stators A, B, and C are given in table III. A photograph of the three stators is presented in figure 1.

Rotor Design

The two rotor blade rows used in this investigation were obtained by using that described in reference 4 and scaling the profile of this rotor to one-half size while maintaining the solidity at 2.86 and the blade height at 2.1 inches. This scaling resulted in a rotor with 74 blades. The 74- and 37-blade rotors with corresponding aspect ratios of 1.46 and 0.73 will be hereafter referred to as rotors A and B, respectively. The aspect ratios and number of blades for these rotors are tabulated in table I. The coordinates for rotors A and B are given in table IV, and the velocity diagrams are given in figure 2. A photograph of the two rotors is presented in figure 3.

APPARATUS, INSTRUMENTATION, AND PROCEDURE

The apparatus, instrumentation, and method of calculating the performance parameters are the same as those described in reference 4 with the following exceptions: (1) A sharp-edged orifice was used to measure air weight flow instead of the submerged adjustable orifice previously used. The sharp-edged orifice was installed in accordance with ASME Power Test Codes and located downstream of an automatic pressure control valve to assure measurements under steady-flow conditions. The sharp-edged orifice was calibrated and found to indicate about 1/2 percent higher weight flow than the previously used submerged orifice. (2) A wire mesh screen was placed about 150 wire diameters upstream of the turbine inlet to remove flow distortion due to large struts and boundary-layer buildup. (3) Another strain-gage torquemeter was used and, although it was statically calibrated, the two torquemeters could differ by as much as 1/2 percent because of dynamic effects which result from manufacturing tolerances.

The difference in level of performance between that reported in reference 3 and that reported herein is attributable to the differences in instrumentation discussed herein and experimental error. A diagrammatic sketch of the cold-air turbine test section is given in figure 4.

The over-all performance of four single-stage turbines was obtained by operating stators A, B, and C with rotor B, and then rotor A with stator A. These turbines will be hereafter referred to as turbines I, II, III, and IV (see table I). Performance test runs were made at constant speeds of 60, 70, 80, 90, 100, 110, and 120 percent design speed. For each speed the total-pressure ratio was varied from approximately 1.8 to the maximum obtainable pressure ratio (approx. 2.5). The turbine-inlet conditions were maintained at approximately 145° F and 32 inches of mercury absolute.

Surveys of total pressure just at the trailing edge and slightly downstream of the exit of the three stators were made to obtain the blade wake characteristics and over-all stator total-pressure ratio.

RESULTS AND DISCUSSION

Effect of Stator and Rotor Aspect Ratio on Over-All Turbine Performance

The over-all performance characteristics obtained in testing the four turbines are presented in figure 5. In this figure equivalent specific work $\Delta h'/\Theta_{cr}$ is plotted against weight-flow - speed parameter $\epsilon w N/\delta$ for lines of constant total-pressure ratio from 1.8 to limiting loading (max. work output). Lines of constant speed as a percent of design speed and constant total efficiency η are also shown.

A comparison of the performance maps for turbines I, II, and III (figs. 5(a), (b), and (c)) indicates that at design equivalent specific work and design equivalent speed the experimentally obtained efficiencies were 0.858, 0.853, and 0.856, respectively. The average of the observed choking weight flow of these three turbines was about 1/2 percent less than design with less than 0.2-percent variation among them. Since the differences in design-point efficiency are small, experimental accuracy of this test setup would tend to obscure any significance that may be attached to these differences. The result to be noted here is that stator aspect ratio was varied from 1.6 to 0.4 with little effect on design-point performance.

A comparison of the performance maps for turbines I and IV (figs. 5(a) and (d)) at design equivalent speed indicates that the experimentally obtained efficiencies were 0.858 and 0.859, respectively. The average choking weight flow was about 0.8 percent less than design with less than 0.2-percent variation. Since the difference in efficiency again is small, it can be concluded that rotor aspect ratio within the range investigated had little effect on design-point performance.

Effect of Stator Aspect Ratio on Stator Wake Characteristics

Stator-mean-section wake characteristics were obtained from total-pressure surveys made just downstream of the trailing edge. Blade wake form factor plotted against outlet critical velocity ratio for the three stators is shown in figure 6. The ratio of blade wake momentum thickness to chord for the three stators is plotted against outlet critical velocity ratio in figure 7. These parameters are similar to those of reference 5, which presents a study of mean-section blade element boundary-layer characteristics. An inspection of figure 6 of the form factor, obtained for the blade wake at the mean radius, indicates that similar

trends were obtained for all three stators. Shown with the form factor is a theoretical variation of form factor with velocity assuming a simple power law velocity profile with an exponent n of 1/7. It can be seen from figure 6 that for stators A and C the experimentally obtained form factor can be closely approximated with the simple power law velocity profile. For stator B, however, most of the points fall somewhat above the theoretical curve, which indicates a somewhat larger displacement thickness.

A comparison of the ratio of momentum thickness to chord in figure 7 indicates a trend of decreasing ratio with velocity and increasing ratio with increasing aspect ratio. This increase in ratio of momentum thickness to chord with aspect ratio is a reflection of the effect of chord Reynolds number on blade element loss.

By using the method of reference 6 the over-all total-pressure ratio across these three stators was computed from the mean-section wake characteristics and is plotted in figure 8 against outlet free-stream critical velocity ratio. This method includes the effects of the end walls by assuming that the mean-section blade element momentum thickness for a straight-back blade is representative of the average momentum thickness on both the blade and end-wall surfaces within the blade passage. Figure 8 shows that the pressure loss increases with increases in exit velocity. Also shown in figure 8 is the momentum-averaged total-pressure ratio obtained from circumferential and radial surveys of total pressure in a segment of the turbine annulus corresponding to one stator blade spacing and in a plane approximately 1/4 inch downstream of the stator trailing edge. The momentum-averaged total-pressure ratios for stators A, B, and C operating at near-design condition are 0.9681, 0.9730, and 0.9671, respectively. A comparison of the momentum-averaged total-pressure ratios with the total-pressure ratios calculated from the mean-section blade element wake characteristics indicates close agreement between the two methods. Further, it is seen that at a critical velocity ratio of 1.10 (approximately design conditions) the total-pressure ratios for stators A, B, and C are 0.9683, 0.9726, and 0.9686, respectively. This variation in total-pressure ratio represents approximately a 14-percent variation in stator loss. On the basis of stator loss alone, it would appear that stator B with an aspect ratio of 0.8 is near the optimum aspect ratio. The effect on turbine performance of this order of change in stator loss, however, is less than 1/2 point in turbine efficiency. Further, it is seen that the total-pressure ratios for stators A and C are about the same on either basis. This indicates that the effect of chord Reynolds number on blade element loss is compensated for by the wall areas, thus yielding comparable total-pressure losses. For stator B the effects of chord Reynolds number and wall area appear to yield the minimum total-pressure loss. However, as pointed out earlier, this difference in total-pressure loss would affect turbine efficiency by less than 1/2 point.

Effect of Rotor Aspect Ratio on Effective Rotor Wake Characteristics

By using the design-point efficiency and the method of reference 7 the effective mean-section two-dimensional momentum thickness was computed. The value of this momentum thickness for rotor A (aspect ratio of 1.46) was 0.0128 and for rotor B (aspect ratio of 0.73) was 0.0117. This variation again is a reflection of the change in chord Reynolds number on blade element loss. Here again, the wall area appears to compensate for the effect of chord Reynolds number to give comparable total-pressure losses and hence comparable over-all turbine efficiency.

CONCLUDING REMARKS

The results of an investigation to determine the effect of stator and rotor aspect ratio on transonic-turbine performance are presented herein. The stator aspect ratios covered were 1.6, 0.8, and 0.4, and all had a solidity of 1.41. The rotor aspect ratios covered were 1.46 and 0.73, and both had a solidity of 2.86. It was found that over-all turbine performance was not affected appreciably by changes in the stator or rotor aspect ratio. Thus, for the range of aspect ratios investigated this result verifies the finding of reference 1, which analytically shows that end-wall area counteracts the effect of chord Reynolds number so that aspect ratio may be varied over a wide range with little effect on over-all performance. The results of this investigation verified these analytical considerations for turbines operating in the transonic flow range.

Lewis Research Center
National Aeronautics and Space Administration
Cleveland, Ohio, November 19, 1958

REFERENCES

1. Miser, James W., Stewart, Warner L., and Whitney, Warren J.: Analysis of Turbomachine Viscous Losses Affected by Changes in Blade Geometry. NACA RM E56F21, 1956.

2. Hauser, Cavour H., and Nusbaum, William J.: Experimental Investigation of Effect of High-Aspect-Ratio Rotor Blades on Performance of Conservatively Designed Turbine. NACA RM E54C18, 1954.

3. Miser, James W., Stewart, Warner L., and Wong, Robert Y.: Effect of a Reduction in Stator Solidity on Performance of a Transonic Turbine. NACA RM E55L09a, 1956.

4. Whitney, Warren J., Monroe, Daniel E., and Wong, Robert Y.: Investigation of Transonic Turbine Designed for Zero Diffusion of Suction-Surface Velocity. NACA RM E54F23, 1954.

5. Whitney, Warren J., Stewart, Warner L., and Miser, James W.: Experimental Investigation of Turbine Stator-Blade-Outlet Boundary-Layer Characteristics and a Comparison with Theoretical Results. NACA RM E55K24, 1956.

6. Stewart, Warner L., Whitney, Warren J., and Wong, Robert Y.: Use of Mean-Section Boundary-Layer Parameters in Predicting Three-Dimensional Turbine Stator Losses. NACA RM E55L12a, 1956.

7. Stewart, Warner L., Whitney, Warren J., and Miser, James W.: Use of Effective Momentum Thickness in Describing Turbine Rotor-Blade Losses. NACA RM E56B29, 1956.

TABLE I. - STATOR AND ROTOR COMBINATIONS

OF TURBINES INVESTIGATED

Turbine	Stator			Rotor		
	Designation	Aspect ratio	Number of blades	Designation	Aspect ratio	Number of blades
I	A	1.6	40	B	0.73	37
II	B	.8	20	B	.73	37
III	C	.4	10	B	.73	37
IV	A	1.6	40	A	1.46	74

TABLE II. - STATOR-BLADE-SECTION COORDINATES

(a) Stator A

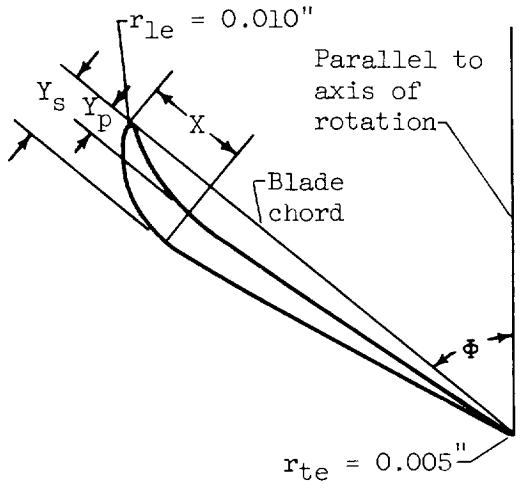

Section	Hub		Mean		Tip	
Φ	53°18'		50°30'		48°50'	
r/r_t	0.70		0.85		1.00	
X, in.	Y_s, in.	Y_p, in.	Y_s, in.	Y_p, in.	Y_s, in.	Y_p, in.
0.00	0.010	0.010	0.010	0.010	0.010	0.010
.10	.116	.056	.124	.051	.104	.048
.20	.165	.086	.176	.080	.152	.072
.30	.185	.096	.195	.092	.171	.078
.40	.184	.096	.192	.094	.171	.076
.50	.167	.092	.174	.090	.159	.072
.60	.145	.084	.154	.084	.143	.068
.70	.123	.074	.135	.076	.127	.064
.80	.100	.062	.114	.069	.112	.058
.90	.078	.050	.094	.060	.096	.052
1.00	.055	.036	.074	.048	.081	.046
1.10	.032	.020	.054	.035	.065	.038
1.20	-----	-----	.034	.020	.050	.030
1.207	.005	.005	-----	-----	-----	-----
1.30	-----	-----	.014	.003	.034	.020
1.314	-----	-----	.005	.005	-----	-----
1.40	-----	-----	-----	-----	.019	.008
1.462	-----	-----	-----	-----	.005	.005

TABLE II. - Continued. STATOR-BLADE-SECTION COORDINATES

(b) Stator B

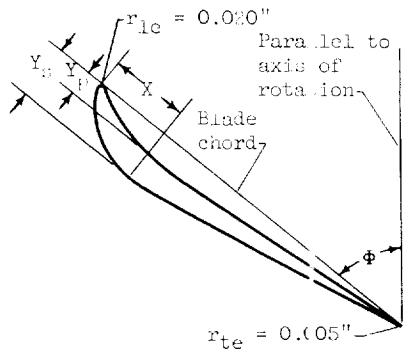

Section	Hub		Mean		Tip	
Φ	53°18'		50°30'		48°50'	
r/r_t	0.70		0.85		1.00	
X, in.	Y_s, in.	Y_p, in.	Y_s, in.	Y_p in	Y_s, in.	Y_p, in.
0.00	0.020	0.020	0.020	0.020	0.020	0.020
.10	.145	.060	.155	.052	.125	.048
.20	.232	.113	.247	.102	.207	.096
.30	.290	.148	.310	.136	.263	.124
.40	.331	.172	.353	.161	.304	.143
.50	.356	.185	.378	.176	.329	.152
.60	.370	.192	.390	.185	.342	.155
.70	.373	.195	.392	.187	.340	.155
.80	.367	.193	.384	.187	.342	.153
.90	.354	.189	.368	.184	.331	.148
1.00	.335	.184	.349	.179	.318	.145
1.10	.313	.176	.329	.174	.300	.141
1.20	.289	.168	.308	.167	.285	.136
1.30	.266	.158	.287	.161	.268	.132
1.40	.243	.147	.266	.153	.253	.128
1.50	.220	.136	.246	.145	.237	.122
1.60	.197	.125	.226	.138	.221	.117
1.70	.174	.112	.205	.129	.205	.110
1.80	.151	.100	.184	.119	.188	.104
1.90	.128	.087	.163	.108	.173	.098
2.00	.103	.071	.141	.096	.157	.091
2.10	.081	.057	.121	.085	.141	.084
2.20	.057	.040	.100	.070	.125	.077
2.30	.034	.021	.079	.054	.109	.069
2.40	.011	.000	.058	.041	.093	.062
2.407	.003	.003	-----	-----	-----	-----
2.50	-----	-----	.037	.024	.076	.050
2.60	-----	-----	.017	.008	.059	.040
2.658	-----	-----	.005	.005	-----	-----
2.70	-----	-----	-----	-----	.044	.027
2.80	-----	-----	-----	-----	.027	.015
2.90	-----	-----	-----	-----	.013	.007
2.93	-----	-----	-----	-----	.008	.005

TABLE II. - Concluded. STATOR-BLADE-SECTION COORDINATES

(c) Stator C

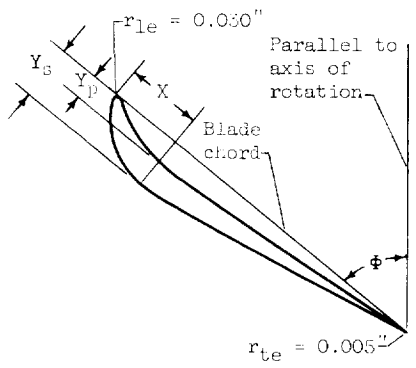

Section	Hub		Mean		Tip	
Φ	53°48'		50°45'		49°10'	
r/r_t	0.70		0.85		1.00	
X, in.	Y_s, in.	Y_p, in.	Y_s, in.	Y_p, in.	Y_s, in.	Y_p, in.
0.00	0.030	0.030	0.030	0.030	0.030	0.030
.20	.200	.112	.310	.097	.253	.095
.40	.455	.209	.490	.191	.405	.174
.60	.568	.275	.614	.260	.515	.227
.80	.642	.317	.685	.306	.586	.260
1.00	.691	.345	.742	.334	.636	.277
1.20	.715	.359	.766	.352	.662	.284
1.40	.719	.363	.766	.359	.666	.284
1.60	.706	.361	.748	.356	.656	.280
1.80	.680	.354	.717	.352	.634	.273
2.00	.642	.343	.678	.348	.605	.268
2.20	.596	.330	.640	.332	.574	.260
2.40	.552	.315	.598	.321	.543	.253
2.60	.506	.295	.556	.303	.506	.244
2.80	.460	.275	.515	.286	.482	.235
3.00	.416	.255	.473	.277	.449	.224
3.20	.370	.235	.431	.262	.416	.216
3.40	.326	.213	.390	.244	.387	.205
3.60	.279	.187	.348	.227	.354	.191
3.80	.233	.161	.308	.207	.323	.180
4.00	.187	.134	.268	.185	.293	.169
4.20	.143	.106	.227	.161	.260	.154
4.40	.097	.075	.185	.134	.229	.141
4.60	.051	.035	.141	.106	.196	.125
4.774	.009	.005	-----	-----	-----	-----
4.80	-----	-----	.101	.077	.148	.102
5.00	-----	-----	.063	.044	.134	.090
5.20	-----	-----	.018	.009	.103	.070
5.334	-----	-----	.000	.000	-----	-----
5.40	-----	-----	-----	-----	.070	.048
5.60	-----	-----	-----	-----	.040	.029
5.786	-----	-----	-----	-----	.009	.009

TABLE III. - TRANSONIC-TURBINE STATOR VELOCITY DIAGRAMS

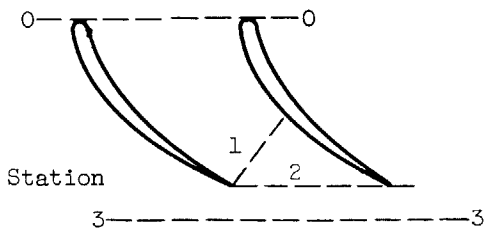

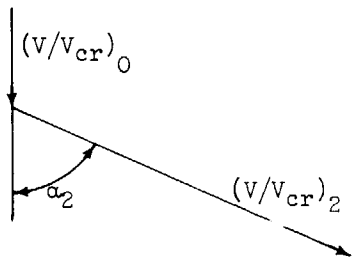

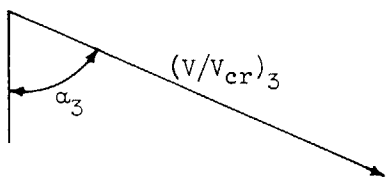

Stator	Aspect ratio	Section	r/r_t	$(V/V_{cr})_0$	$(V/V_{cr})_2$	$(V/V_{cr})_3$	α_2, deg	α_3, deg
A	1.6	Hub	0.70	0.291	1.302	1.293	65.8	66.7
		Mean	.85	.291	1.110	1.104	61.8	62.4
		Tip	1.00	.291	.984	.976	57.7	58.4
B	0.8	Hub	0.70	0.291	1.297	1.293	66.3	66.7
		Mean	.85	.291	1.107	1.104	62.1	62.4
		Tip	1.00	.291	.980	.976	58.1	58.4
C	0.4	Hub	0.70	0.291	1.295	1.293	66.5	66.7
		Mean	.85	.291	1.105	1.104	62.3	62.4
		Tip	1.00	.291	.977	.976	58.3	58.4

TABLE IV. - ROTOR-BLADE-SECTION COORDINATES

(a) Rotor A

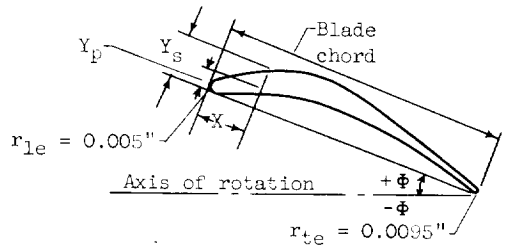

Section	Hub		Mean		Tip	
Φ, deg	-3.25		7.93		19.87	
r/r_t	0.70		0.85		1.00	
X, in.	Y_s, in.	Y_p, in.	Y_s, in.	Y_p, in.	Y_s, in.	Y_p, in.
0.000	0.005	0.005	0.005	0.005	0.005	0.005
.050	.071	.044	.069	.041	.058	.031
.100	.129	.091	.128	.084	.107	.062
.150	.183	.132	.179	.120	.149	.088
.200	.233	.169	.225	.152	.186	.112
.250	.278	.200	.267	.180	.218	.132
.300	.319	.228	.303	.203	.244	.150
.350	.355	.252	.333	.222	.266	.165
.400	.385	.273	.358	.237	.283	.179
.450	.410	.291	.376	.249	.297	.190
.500	.429	.305	.389	.259	.306	.199
.550	.442	.316	.396	.267	.312	.206
.600	.451	.326	.399	.272	.315	.212
.650	.454	.333	.398	.274	.316	.215
.700	.452	.338	.392	.274	.313	.217
.750	.446	.338	.383	.272	.307	.215
.800	.435	.335	.369	.267	.298	.212
.850	.420	.327	.352	.259	.286	.206
.900	.400	.315	.332	.248	.271	.198
.950	.377	.300	.309	.235	.254	.188
1.000	.348	.280	.283	.219	.235	.177
1.050	.316	.257	.255	.202	.216	.164
1.100	.281	.230	.226	.181	.195	.149
1.150	.243	.199	.196	.158	.173	.134
1.200	.203	.165	.165	.133	.152	.117
1.250	.163	.129	.134	.107	.130	.100
1.300	.121	.091	.103	.078	.109	.082
1.350	.080	.052	.072	.048	.087	.063
1.400	.038	.013	.041	.018	.066	.044
1.429	.010	.010	-----	-----	-----	-----
1.443	-----	-----	.010	.010	-----	-----
1.450	-----	-----	-----	-----	.044	.023
1.500	-----	-----	-----	-----	.023	.002
1.510	-----	-----	-----	-----	.010	.010

TABLE IV. - Concluded. ROTOR-BLADE-SECTION COORDINATES

(b) Rotor B

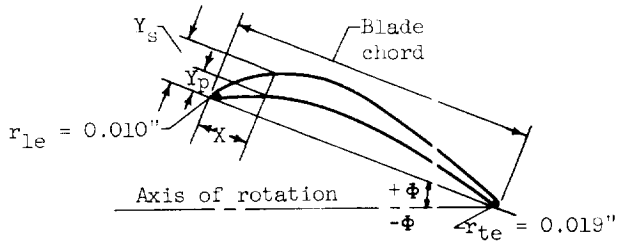

Section	Hub		Mean		Tip	
Φ, deg	-3.25		7.93		19.87	
r/r_t	0.70		0.85		1.00	
X, in.	Y_s, in.	Y_p, in.	Y_s, in.	Y_p, in.	Y_s, in.	Y_p, in.
0.000	0.010	0.010	0.010	0.010	0.010	0.010
.100	.142	.088	.138	.08_	.116	.061
.200	.257	.182	.255	.16'	.213	.123
.300	.365	.264	.357	.240	.297	.176
.400	.465	.337	.449	.304	.371	.223
.500	.555	.400	.534	.359	.435	.264
.600	.637	.455	.606	.405	.487	.299
.700	.710	.504	.666	.443	.531	.330
.800	.770	.546	.715	.474	.566	.357
.900	.819	.581	.752	.493	.593	.379
1.000	.857	.609	.777	.513	.612	.397
1.100	.884	.632	.792	.533	.623	.412
1.200	.901	.651	.798	.543	.630	.423
1.300	.908	.666	.795	.547	.631	.430
1.400	.904	.675	.784	.547	.625	.433
1.500	.892	.676	.765	.543	.613	.430
1.600	.870	.669	.738	.533	.595	.423
1.700	.839	.653	.703	.517	.571	.412
1.800	.800	.630	.663	.496	.541	.396
1.900	.753	.599	.617	.469	.507	.376
2.000	.696	.560	.565	.438	.470	.353
2.100	.632	.513	.510	.403	.431	.327
2.200	.561	.459	.452	.362	.389	.298
2.300	.486	.398	.391	.316	.346	.267
2.400	.406	.330	.329	.266	.303	.234
2.500	.325	.258	.267	.213	.260	.199
2.600	.242	.182	.205	.156	.217	.163
2.700	.159	.104	.143	.096	.174	.126
2.800	.076	.025	.081	.035	.131	.087
2.858	.019	.019	-----	-----	-----	-----
2.885	-----	-----	.019	.019	-----	-----
2.900	-----	-----	-----	-----	.088	.046
3.000	-----	-----	-----	-----	.045	.004
3.032	-----	-----	-----	-----	.019	.019

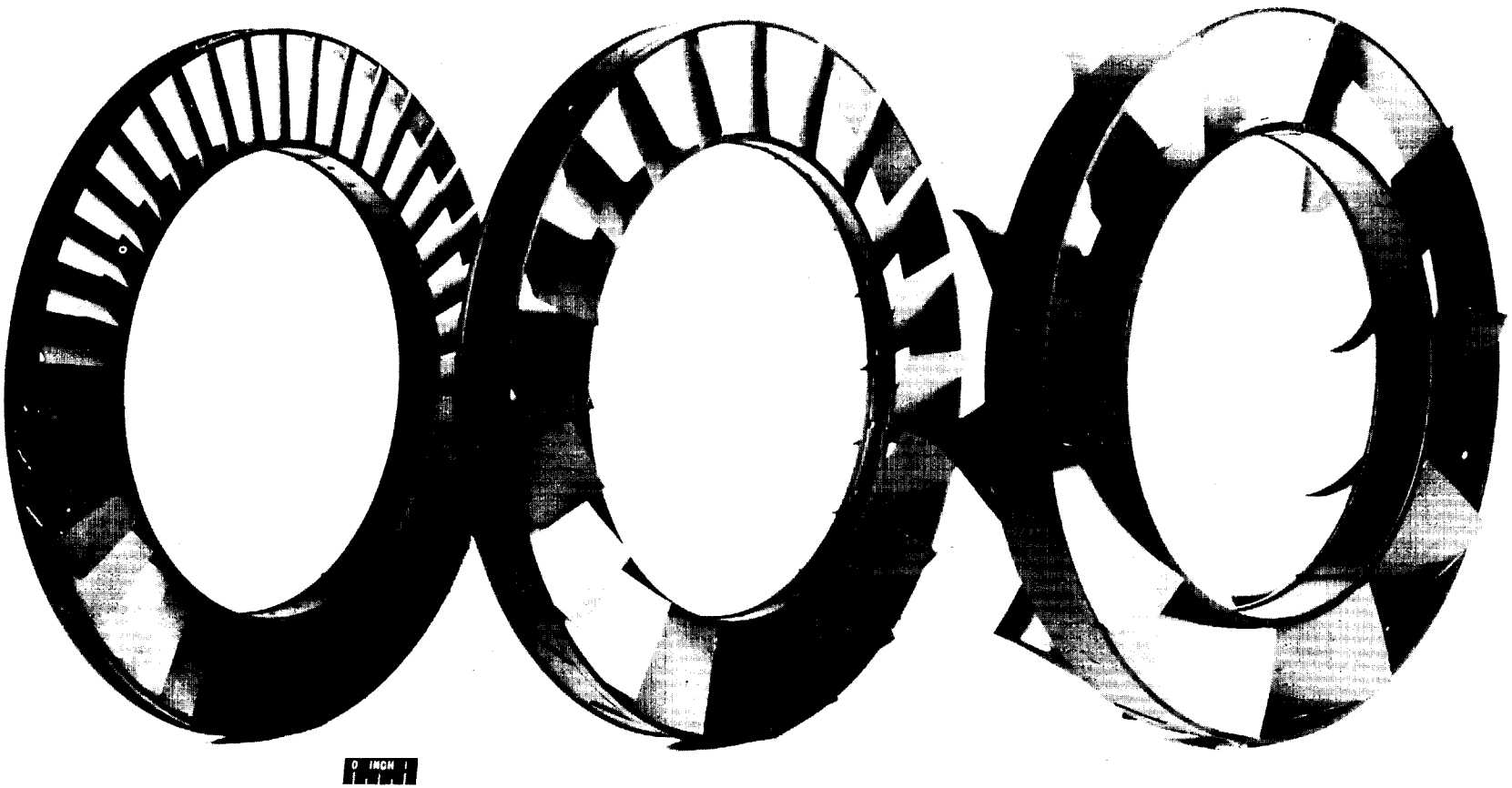

Stator A Stator B Stator C

C-48499

Figure 1. - Transonic-turbine stator assembly.

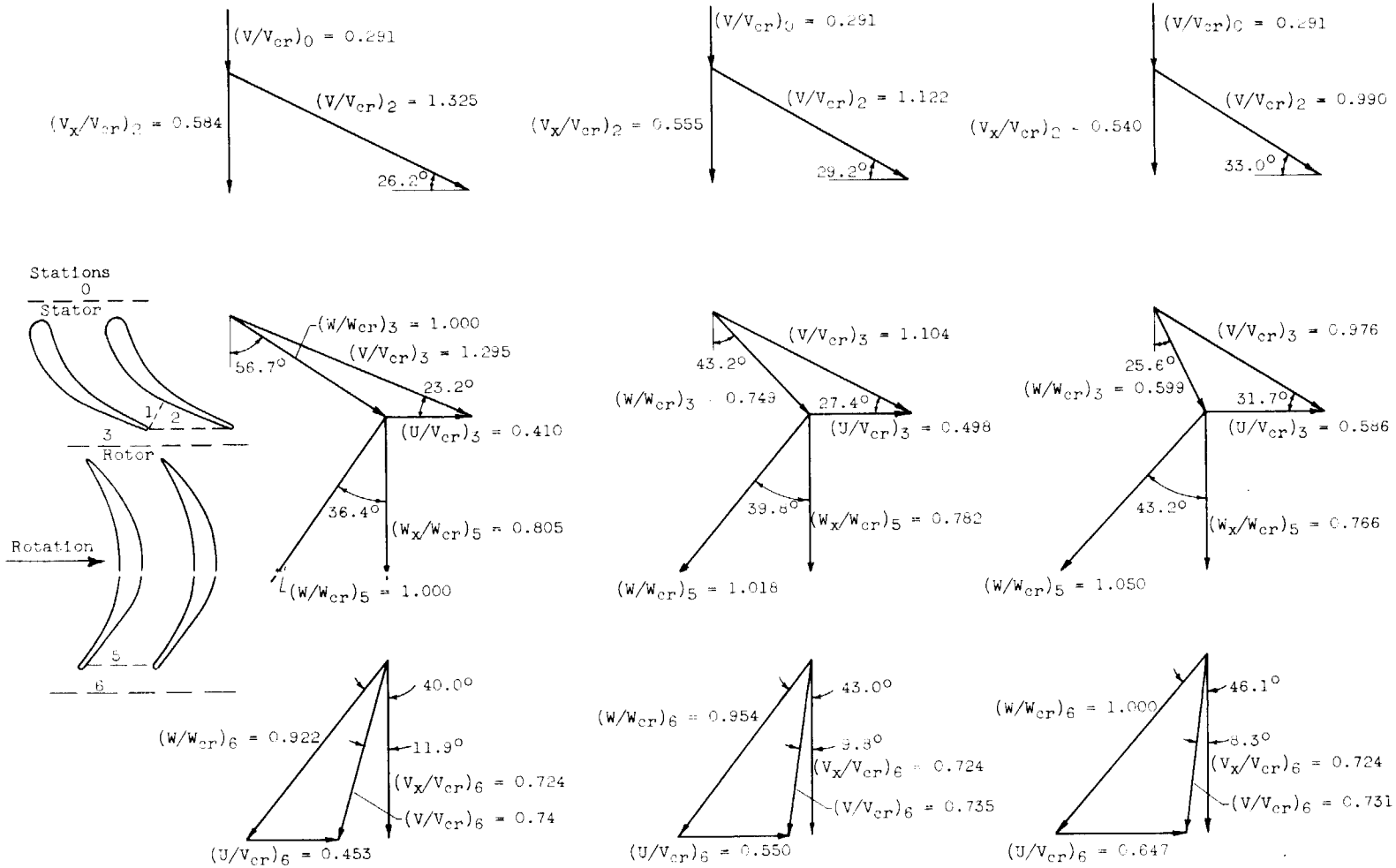

(a) Hub; r/r_t, 0.70. (b) Mean; r/r_t, 0.85. (c) Tip; r/r_t, 1.00.

Figure 2. - Transonic-turbine velocity diagrams. Rotors A and B with stator A.

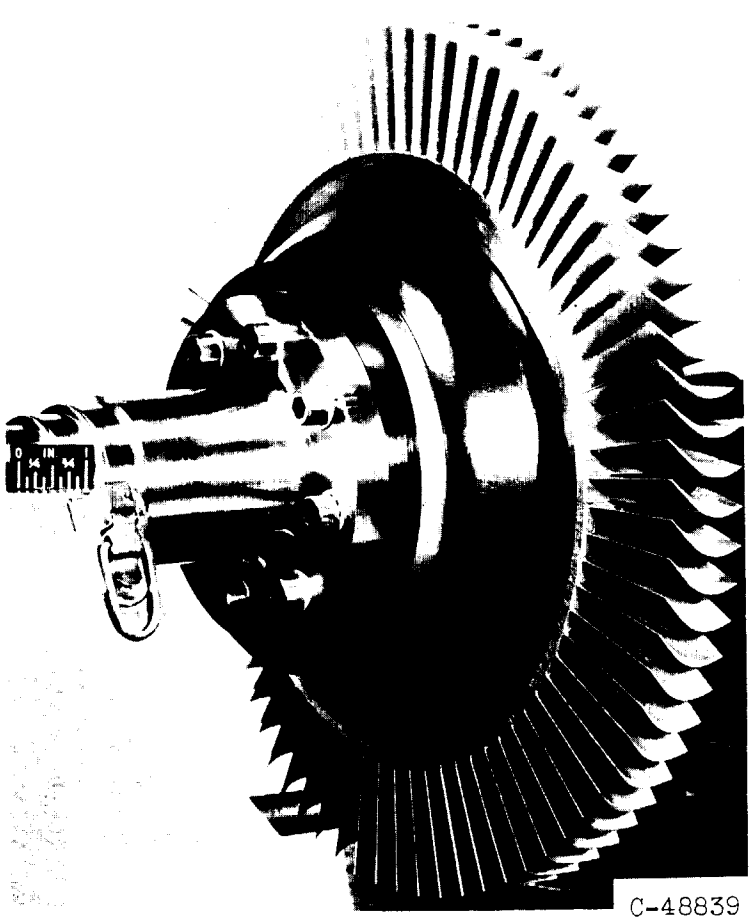

C-48839

Rotor A

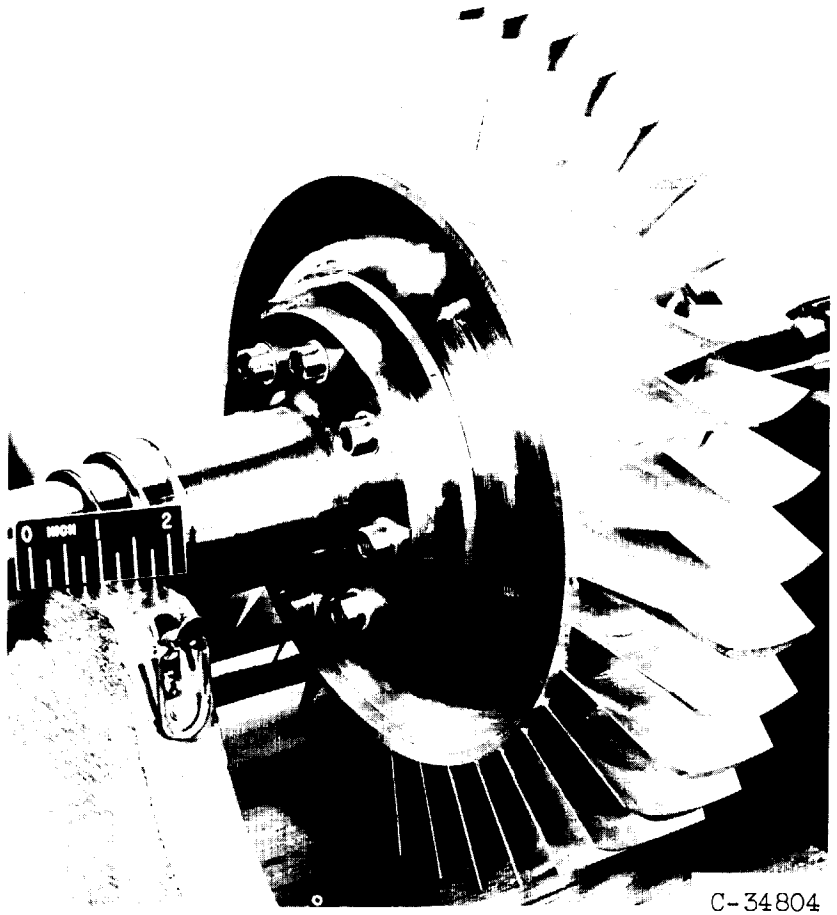

C-34804

Rotor B

Figure 3. - Transonic rotor assemblies.

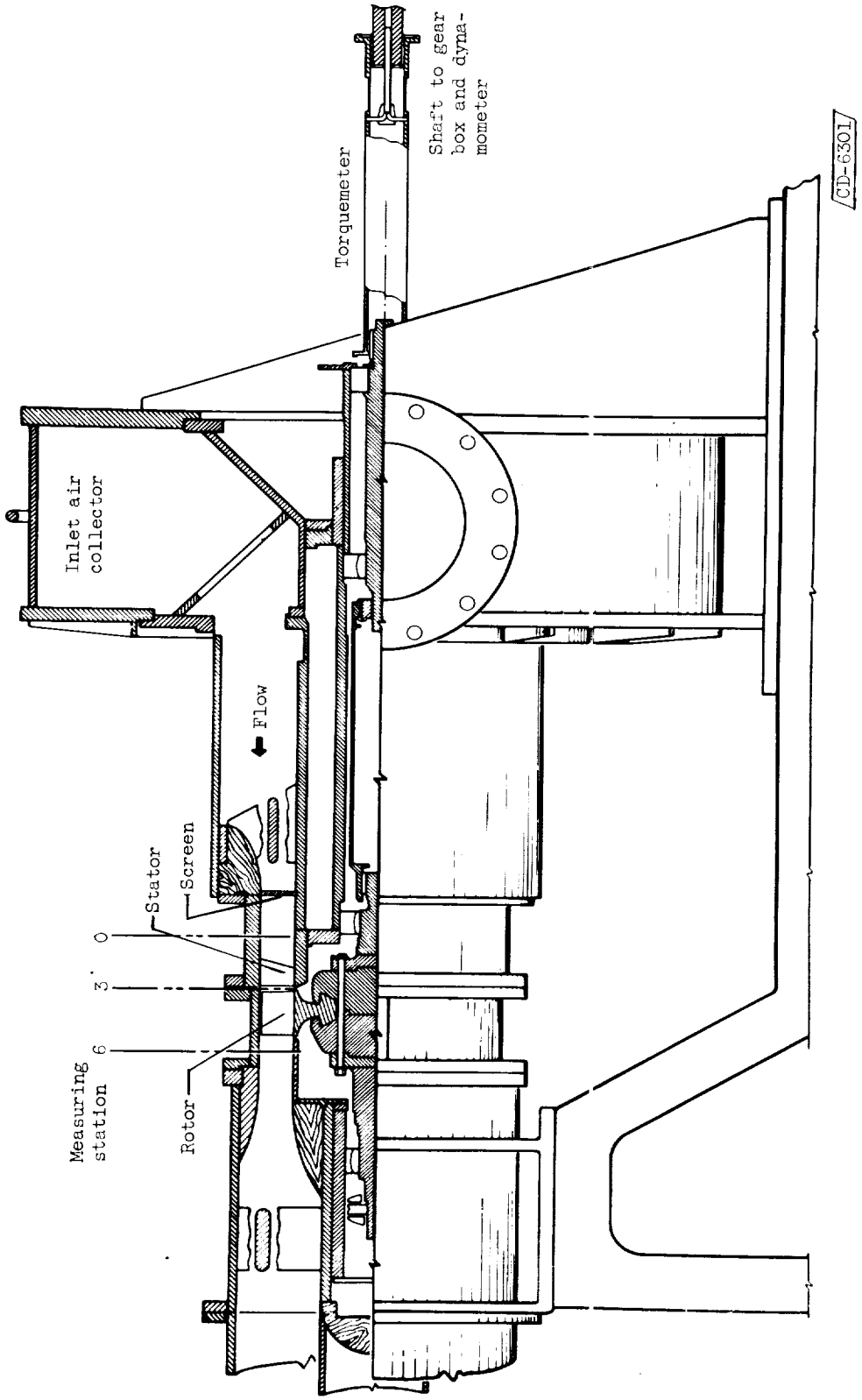

Figure 4. - Diagrammatic sketch of cold-air turbine test section.

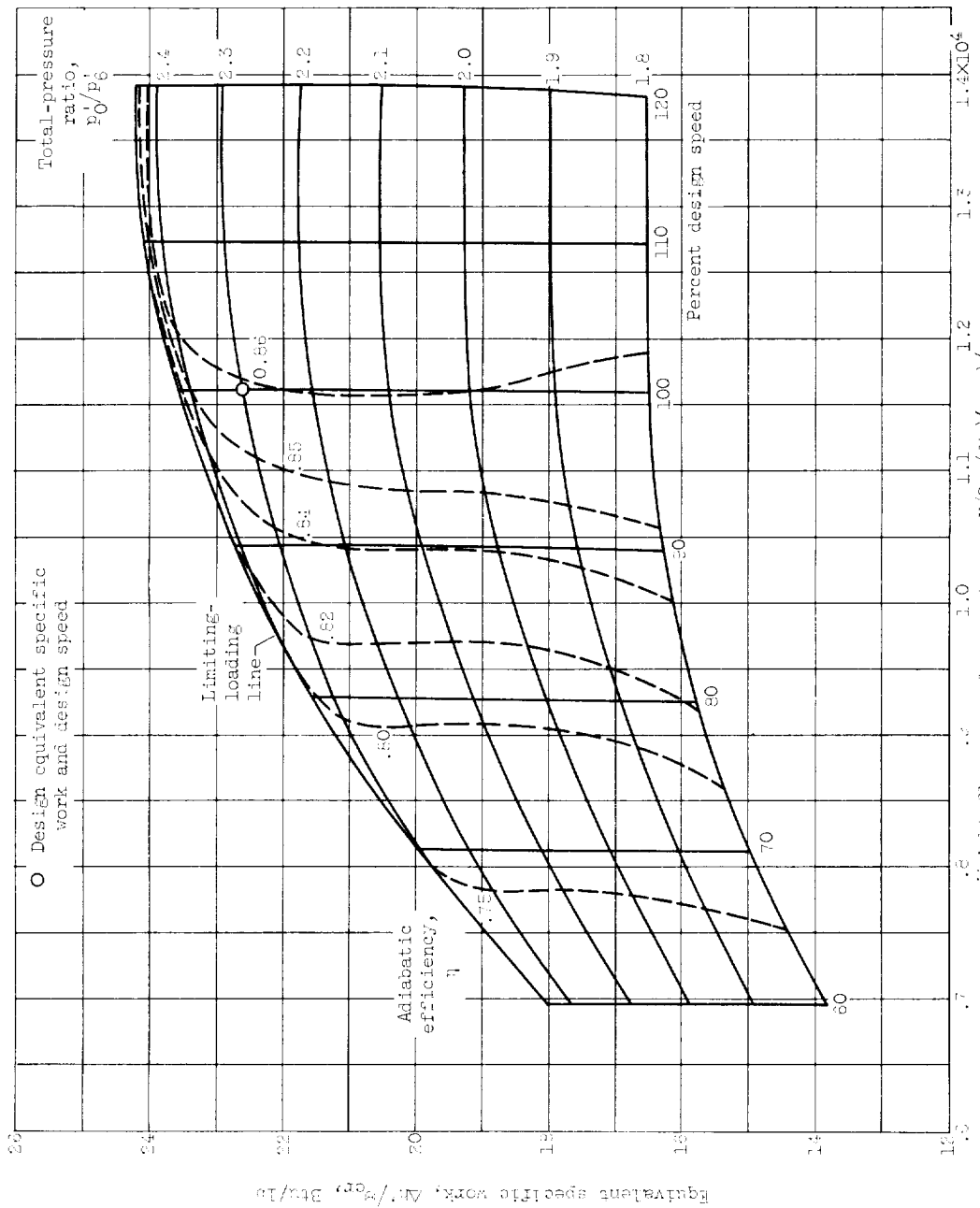

(a) Turbine I.

Figure 5. - Over-all turbine performance (see table I).

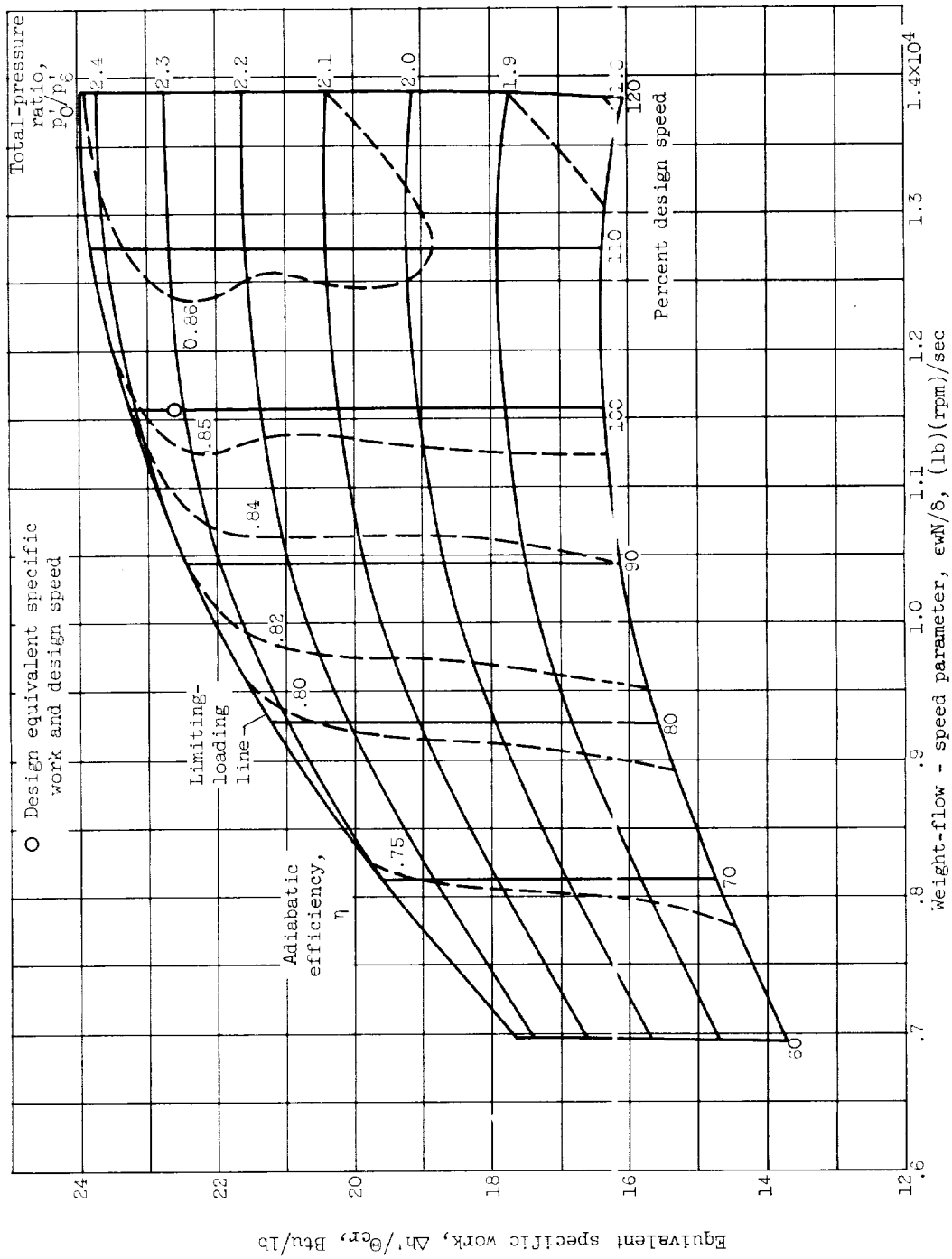

(b) Turbine II.

Figure 5. - Continued. Over-all turbine performance (see table I).

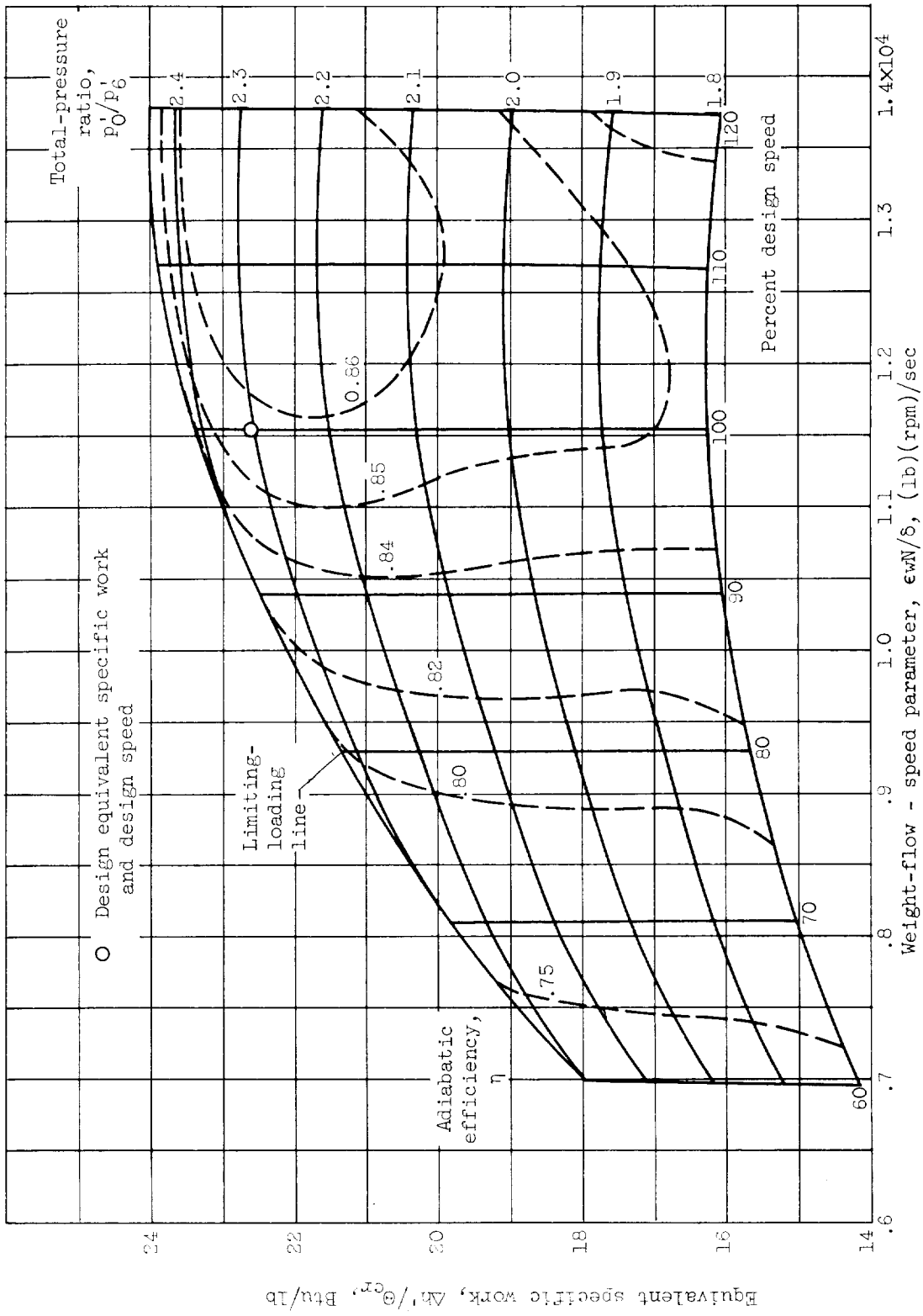

(c) Turbine III.

Figure 5. - Continued. Over-all turbine performance (see table I).

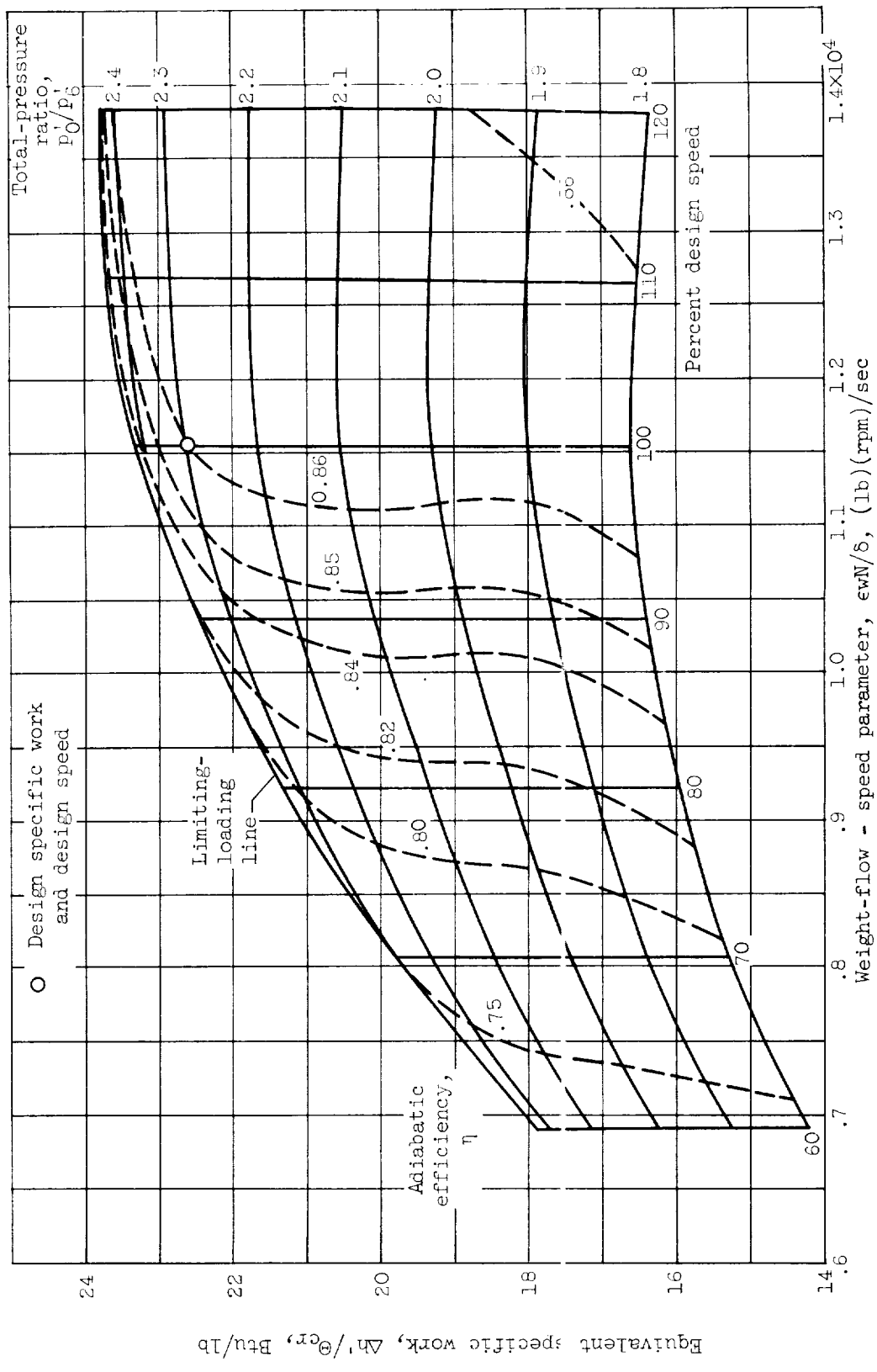

(d) Turbine IV.

Figure 5. - Concluded. Over-all turbine performance (see table I).

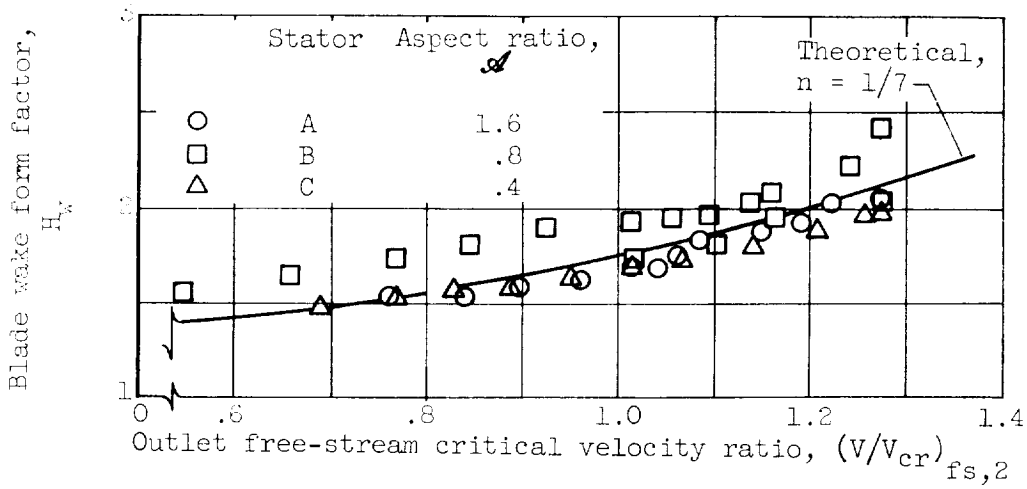

Figure 6. - Variation of blade wake characteristics with stator-outlet free-stream critical velocity ratio.

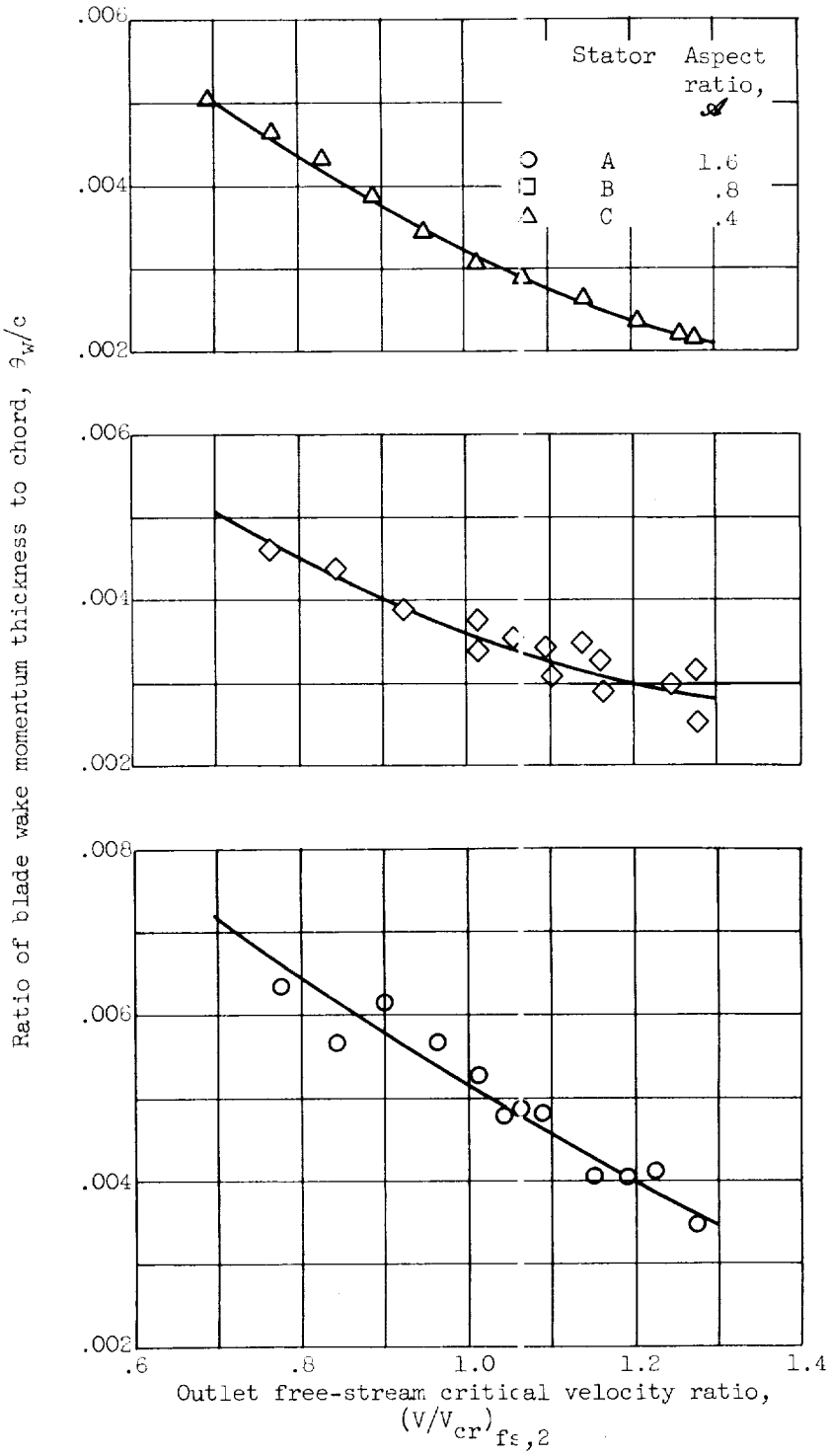

Figure 7. - Variation of ratio of mean-section blade wake momentum thickness to chord with outlet free-stream critical velocity ratio for three transonic-turbine stators.

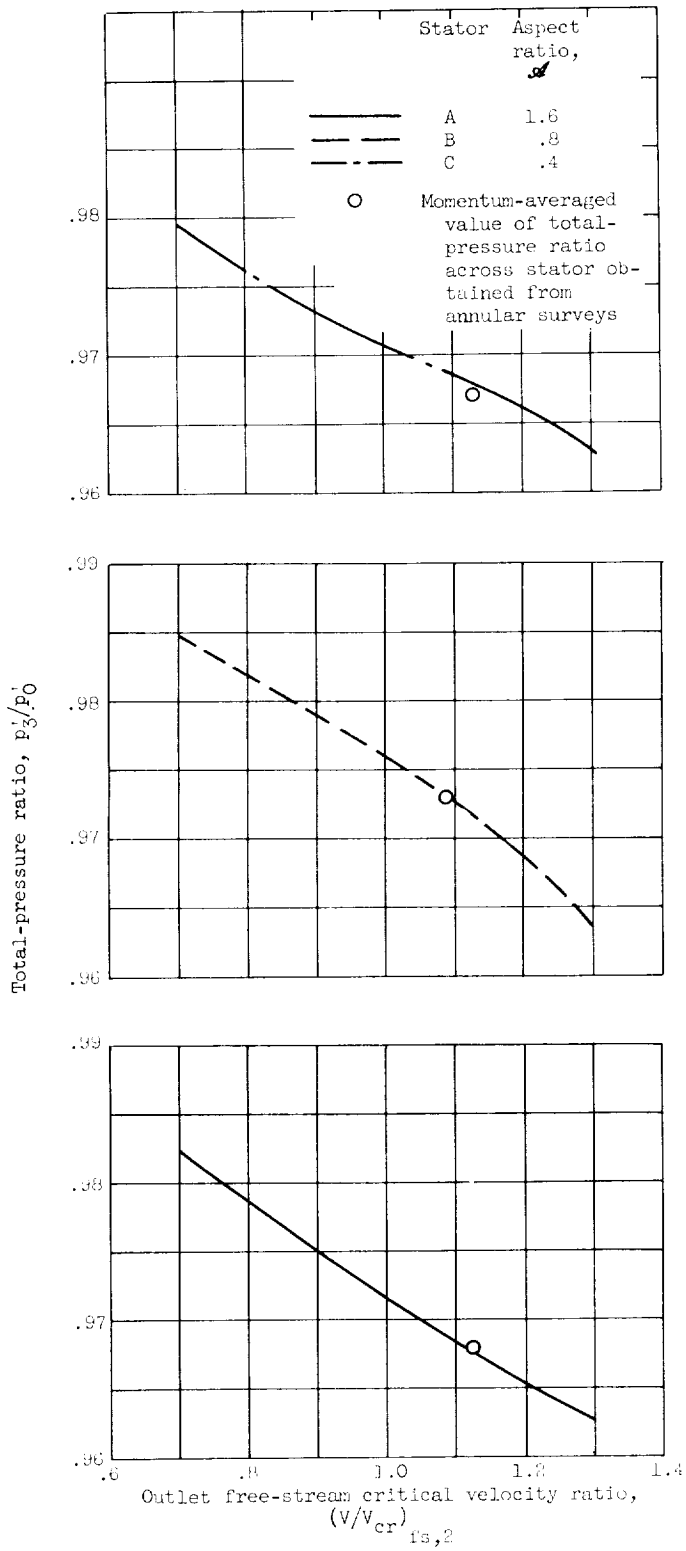

Figure 8. - Variation in total-pressure ratio across stator with blade-outlet critical velocity ratio based on experimentally obtained values of momentum thickness at mean-section trailing edge.